

1-1-1972

A study of the frequency domain polarity correlation technique of reactor noise analysis

Rick Lynn Hannen
Iowa State University

Follow this and additional works at: <https://lib.dr.iastate.edu/rtd>

 Part of the [Engineering Commons](#)

Recommended Citation

Hannen, Rick Lynn, "A study of the frequency domain polarity correlation technique of reactor noise analysis" (1972). *Retrospective Theses and Dissertations*. 17487.
<https://lib.dr.iastate.edu/rtd/17487>

This Thesis is brought to you for free and open access by the Iowa State University Capstones, Theses and Dissertations at Iowa State University Digital Repository. It has been accepted for inclusion in Retrospective Theses and Dissertations by an authorized administrator of Iowa State University Digital Repository. For more information, please contact digirep@iastate.edu.

A study of the frequency domain
polarity correlation technique
of reactor noise analysis

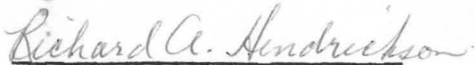
by

Rick Lynn Hannen

Submitted to the
Graduate Faculty in Partial Fulfillment of
The Requirements for the Degree of
MASTER OF ENGINEERING

Major Subject: Nuclear Engineering

Approved:


In Charge of Major Work


For the Major Department

Iowa State University
Ames, Iowa

1972

TABLE OF CONTENTS

	<u>Page</u>
I. INTRODUCTION	1
II. THEORY OF THE COHERENCE FUNCTION RELATIONSHIP WITH THE PROMPT NEUTRON DECAY CONSTANT	4
A. Background	4
B. Reactor Noise Source	5
C. Reactor Transfer Function	8
D. Auto Spectral Densities	12
E. Cross Spectral Density	17
F. Coherence Function	20
III. DETERMINATION OF THE COHERENCE FUNCTION BY POLARITY CORRELATION	23
A. Overall System	23
B. Theory of Coherence Function Determination	25
IV. APPLICATION OF DYNAMIC FILTERING	28
A. Theory of Dynamic Filtering	28
B. Advantages of Dynamic Filtering	35
C. Requirements of a Polarity Correlation Filtering System	35
V. CONCLUDING REMARKS	37
VI. BIBLIOGRAPHY	39
VII. ACKNOWLEDGMENTS	41

I. INTRODUCTION

The basis for reactor noise analysis is the comparison of the output noise signal to the assumed or known input noise signal to observe how the reactor has modified the signal. The applicable kinetic model of the reactor is then used to determine what the relationship between the various reactor parameters must be in order to modify the signal in the way that has been observed.

The above method is the basic method of reactor noise analysis, but the implementation of this basic method is quite varied. Many options and combinations of options are available to the designer of a reactor noise analysis system.

One option is the choice of input signal. Experiments by Balcomb [2], Stern [22], and Valat [24] used externally applied signals. Other experiments such as those of Cohn [8], Danofsky [10], and Seifritz, et al. [21], relied on the natural stochastic processes of fission and capture for the random noise input signal with no externally applied input. When externally applied signals are used, care must be taken to insure that the perturbations introduced are small enough to preserve system linearity. Linear formulations of reactor transfer functions are valid for small signal analysis only.

The second option in noise analysis methods is the choice of analyzing the signals in the frequency or the time domain. Balcomb, et al. [3], Dragt [13], and Rajagopal [17] performed experiments in the time domain, while Badgley, et al. [1] and Seifritz [19] conducted

investigations in the frequency domain. In either case the results can be transformed to the other domain by use of the Fourier transform or its inverse,

$$F(\omega) = \int_{-\infty}^{\infty} f(t)e^{-j\omega t} dt, \quad (1)$$

or

$$f(t) = \frac{1}{2\pi} \int_{-\infty}^{\infty} F(\omega)e^{+j\omega t} d\omega. \quad (2)$$

The third option of the experimenter in reactor noise analysis is the number of detection channels to be used. Early experiments by Balcomb, et al. [3], Cohn [8], and Rajagopal [17] used only one detection system to determine the output signal. Use of only one detection system requires that the detector efficiency be high enough to make the reactor noise signal observable above the random detection noise. The efficiency requirement can be relaxed somewhat by the use of two detection channels. Cross correlation of the signals from these two channels enhances the signal and rejects the uncorrelated noise. This type of cross correlation was used in investigations by Kryter, et al. [15] and Seifritz, et al. [20]. It should be emphasized that the cross correlation discussed here is between detection channels and not between input and output signals. References to both of these applications of cross correlation are found in the literature.

Recently the use of the polarity correlation technique in reactor noise analysis has received much attention. In the polarity correlation process only the signs of the signals, with respect to

their mean values, are correlated. Theoretical investigations by Pacilio [16] and experimental investigations by Dragt [12] and Seifritz [19] have demonstrated that the polarity of the signals contains sufficient information to allow reactor noise to be analyzed by this method.

Of the many possible combinations of options listed above, the objective of this study is to explore the theory and method of implementation of only one combination of these options, namely, the frequency domain polarity correlation method using two detection channels and an input of natural stochastic process noise. The theory will be developed to determine the prompt neutron decay constant for a critical reactor. The method of implementation will be presented as a method similar to that of Seifritz [19], but modified by the use of dynamic (heterodyne) filtering.

II. THEORY OF THE COHERENCE FUNCTION RELATIONSHIP WITH THE PROMPT NEUTRON DECAY CONSTANT

A. Background

In the following sections formulations of the reactor noise source, the reactor transfer function, and the auto and cross spectral densities are developed for the critical reactor to show how the coherence function relates to the prompt neutron decay constant, α_c . The prompt neutron decay constant is defined as

$$\alpha_c = \beta/\ell = \beta v \Sigma_A ,$$

where β is the delayed neutron fraction,

ℓ is the prompt neutron lifetime,

Σ_A is the total macroscopic absorption cross section for thermal neutrons, and

v is the thermal neutron velocity.

The polarity correlation technique for determining the coherence function is then developed to complete the theory of determining α_c by polarity correlation.

In this investigation it is assumed that the reader has knowledge of the basic concepts of impulse response, convolution, transfer functions, correlation functions and the Fourier transforms of correlation functions, viz, the spectral density functions. All of these concepts are discussed in texts by Bendat [4], Brown, et al. [6], and Uhrig [23].

B. Reactor Noise Source

The noise input signal arising from the stochastic processes of fission and capture was first formalized into the noise-equivalent neutron source model by Cohn [9]. A condensed form of this development is given below.

Since both the fission and capture processes obey Poisson statistics, the same statistics obeyed by random electron flow in a diode, the noise-equivalent neutron source may be obtained from the Schottky formula [11] originally developed as a model of random electron flow in a diode. The analogous formula for calculating the noise-equivalent neutron source may be written as

$$N_{ns}(\omega) = 2 \sum_i q_i^2 \bar{r}_i, \quad (3)$$

where $N_{ns}(\omega)$ is the noise-equivalent neutron power spectral density in neutrons²/sec,

q_i is the net number of neutrons produced in the occurrence of a reaction of type i , and

\bar{r}_i is the average rate of occurrence of the i type of reaction in units of inverse seconds.

To apply equation (3), q and \bar{r} must be determined for the capture process and for each fission process which results in a different number of neutrons being emitted. If η is the neutron density in the reactor, l is the prompt neutron lifetime defined as $l = 1/(v\Sigma_A)$, Σ_c is the macroscopic capture cross section, and Σ_f is the macroscopic

fission cross section, then on a unit volume basis η/ℓ is the total reaction rate with

$$(\eta/\ell) \frac{\Sigma_c}{\Sigma_c + \Sigma_F} \quad (4)$$

the capture rate, and

$$(\eta/\ell) \frac{\Sigma_F}{\Sigma_c + \Sigma_F} \quad (5)$$

the total fission rate. Defining P_ν as the probability that ν neutrons will be emitted during fission, the individual neutron production rates become

$$(\eta/\ell) \frac{P_\nu \Sigma_F}{\Sigma_c + \Sigma_F} . \quad (6)$$

The net number of neutrons produced is minus one for the capture process, and $\nu - 1$ for the various fission processes. When the net number of neutrons produced, q_i , and the average rate of occurrence, \bar{r}_i , for all of the processes are inserted into equation (3) the result is

$$N_{ns}(\omega) = \frac{2\eta}{\ell(\Sigma_c + \Sigma_F)} \left[\Sigma_c + \Sigma_F \sum_{\nu=1}^{\infty} (\nu - 1)^2 P_\nu \right], \quad (7)$$

where

$$\sum_{\nu=1}^{\infty} (\nu - 1)^2 P_\nu = \sum_{\nu=1}^{\infty} \nu^2 P_\nu - 2 \sum_{\nu=1}^{\infty} \nu P_\nu + \sum_{\nu=1}^{\infty} P_\nu . \quad (8)$$

From the definition of P the following equations hold:

$$\sum_{\nu=1}^{\infty} P_\nu = 1 \quad (9)$$

$$\sum_{\nu=1}^{\infty} \nu^p \nu = \bar{\nu} \quad (10)$$

$$\sum_{\nu=1}^{\infty} \nu^2 \nu = \bar{\nu}^2 . \quad (11)$$

In addition, the equation

$$\frac{\bar{\nu} \Sigma_F}{\Sigma_c + \Sigma_F} = 1 \quad (12)$$

must hold in an infinite reactor, since the average number of neutrons emitted per fission times the total fission rate must equal the sum of the total fission rate and the capture rate. Equation (7) now becomes

$$\begin{aligned} N_{ns}(\omega) &= \frac{2\eta}{\ell} \left[1 + \frac{1}{\bar{\nu}} (\bar{\nu}^2 - 2\bar{\nu}) \right] \\ &= \frac{2\eta}{\ell} \left[\frac{\bar{\nu}^2 - \bar{\nu}}{\bar{\nu}} \right] = \frac{2\eta \bar{\nu} D}{\ell} \end{aligned} \quad (13)$$

where

$$D = \frac{\bar{\nu}^2 - \bar{\nu}}{\bar{\nu}^2} \quad (14)$$

is the Diven factor.

Since a reactivity change, δk , results in a change of $\delta k(\eta/\ell)$ in the neutron production rate, the noise-equivalent reactivity source spectral density, with dimensions compatible to the standard reactor transfer function, can be written as

$$\begin{aligned} \phi_{nn}(\omega) &= (\ell/n)^2 N_{ns}^2(\omega) \\ &= \frac{2\ell \bar{\nu} D}{\eta} . \end{aligned} \quad (15)$$

It should be noted that $\bar{\phi}_{nn}(\omega)$ is independent of the frequency variable, ω , and is therefore a "white" or "Gaussian" noise source.

C. Reactor Transfer Function

The reactor transfer function, $H_r(\omega)$, is the frequency domain description of the kinetics of a reactor model. In this study the point kinetic model of a critical reactor is developed in a manner similar to that used by Glasstone, et al. [14]. This model does not account for spatial variations within the reactor.

The development starts with the well-known diffusion equation,

$$D\nabla^2\phi(t) - \Sigma_A\phi(t) + S(t) = \frac{d\eta(t)}{dt}, \quad (16)$$

where

D is the diffusion coefficient,

$\phi(t)$ is the time dependent neutron flux in neutrons/cm²-sec,

$S(t)$ is the time dependent neutron source in neutrons/cm³-sec,

Σ_A is the average macroscopic absorption cross section of the reactor, and

η is the neutron density in cm⁻³.

The total neutron production rate is $K_\infty\Sigma_A\phi(t)$, of which $\beta K_\infty\Sigma_A\phi(t)$ is the delayed neutron production rate and $(1 - \beta)K_\infty\Sigma_A\phi(t)$ is the prompt neutron production rate, where β is the delayed neutron fraction and K_∞ is the infinite reactor multiplication factor. With the use of the one group model of delayed neutrons, the delayed neutron production rate can also be defined as $\lambda C(t)$, where λ is the decay constant in sec⁻¹, and $C(t)$ is the precursor concentration in cm⁻³.

When the source term is replaced by the delayed and prompt neutron production rates, equation (16) becomes

$$D\nabla^2\phi(t) - \Sigma_A\phi(t) + (1 - \beta)K_\infty\Sigma_a\phi(t) + \lambda C(t) = \frac{d\eta(t)}{dt} . \quad (17)$$

Provided the reactor is near critical $\nabla^2\phi(t)$ can be replaced by $-B^2\phi(t)$, resulting in

$$K_\infty v\Sigma_A \left[(1 - \beta) - \frac{1 + B^2 L^2}{K_\infty} \right] \eta(t) + \lambda C(t) = \frac{d\eta(t)}{dt} , \quad (18)$$

where $L^2 = D/\Sigma_A$ and $\phi(t) = v\eta(t)$. For the one group model

$$K_{\text{eff}} = \frac{K_\infty}{1 + B^2 L^2} , \quad (19)$$

leaving

$$K_\infty v\Sigma_A \left[1 - \beta - \frac{1}{K_{\text{eff}}} \right] \eta(t) + \lambda C(t) = \frac{d\eta(t)}{dt} . \quad (20)$$

Noting that the prompt neutron lifetime is equal to the neutron mean free path divided by the neutron velocity ($\ell = 1/\Sigma_A v$), and that δk is defined as

$$\delta k = K_{\text{eff}} - 1, \quad (21)$$

equation (20) may be written as

$$\frac{d\eta(t)}{dt} = \left(\frac{\delta k}{\ell} - \beta \right) \eta(t) + \lambda C(t). \quad (22)$$

An independent expression containing $C(t)$ and $\eta(t)$ is required to solve for these two variables. The rate of change of $C(t)$ may be described as the precursor production rate minus the decay rate,

$$\frac{dC(t)}{dt} = \beta K_{\infty} \sum_A \phi(t) - \lambda C(t). \quad (23)$$

Substituting $\phi(t) = v\eta(t)$ and $\ell = 1/v\sum_A$ results in

$$\frac{dC(t)}{dt} = \left(\frac{\beta}{\ell}\right)\eta(t) - \lambda C(t). \quad (24)$$

Addition of equations (22) and (24) yields

$$\frac{d\eta(t)}{dt} = \frac{\delta k}{\ell} \eta(t) - \frac{dC(t)}{dt}. \quad (25)$$

Assuming only small variations from steady state conditions, $C(t)$

and $\eta(t)$ can be written as

$$C(t) = C + \delta C(t) \quad (26)$$

and

$$\eta(t) = \eta + \delta\eta(t). \quad (27)$$

Hence, equation (25) becomes

$$\frac{d\eta(t)}{dt} = \frac{d(\delta\eta(t))}{dt} = \frac{\delta k}{\ell} (\eta + \delta\eta(t)) - \frac{d(\delta C(t))}{dt}, \quad (28)$$

or ignoring the small $\delta k \delta\eta(t)$ term

$$\frac{d(\delta\eta(t))}{dt} = \frac{\delta k}{\ell} \eta - \frac{d(\delta C(t))}{dt}. \quad (29)$$

Equation (24) becomes

$$\frac{dC(t)}{dt} = \frac{d(\delta C(t))}{dt} = \frac{\beta}{\ell} (\eta + \delta\eta(t)) - \lambda(C + \delta C(t)). \quad (30)$$

In a steady state condition $dC(t)/dt = 0$, $\delta\eta(t) = 0$, and $\delta C(t) = 0$

resulting in the equation

$$\frac{\beta}{\ell} \eta = \lambda C. \quad (31)$$

Using equation (31), equation (30) reduces to

$$\frac{d(\delta C(t))}{dt} = \frac{\beta}{\ell} \delta \eta(t) - \lambda \delta C(t). \quad (32)$$

Equations (29) and (32) can be transformed from the time domain to the frequency domain by use of the Laplace transform where $j\omega$ is the Laplace variable, so that

$$j\omega \delta \eta(j\omega) = \frac{\eta}{\ell} \delta k - j\omega \delta C(j\omega) \quad (33)$$

and

$$j\omega \delta C(j\omega) = \frac{\beta}{\ell} \delta \eta(j\omega) - \lambda \delta C(j\omega). \quad (34)$$

Combining these last two equations, and noting that δk may be a function of frequency, yields the one group critical reactor transfer function

$$H_r(\omega) = \frac{\delta \eta(j\omega)}{\delta k(\omega)} = \frac{\eta}{j\omega \ell + \frac{j\omega \beta}{j\omega + \lambda}}. \quad (35)$$

When the delayed neutron effects are ignored by setting $\lambda = 0$, the transfer function becomes

$$H_r(\omega) = \frac{\eta}{j\omega \ell + \beta} = \frac{\eta/\beta}{1 + j\omega/\alpha_c} \quad (36)$$

where the prompt neutron decay constant, α_c , is equal to β/ℓ .

D. Auto Spectral Densities

The signal flow diagram resulting in two signals $x(t)$ and $y(t)$, the outputs of two independent but identical detection channels, is shown in Figure 1. With the use of the convolution integral the signal $b(t)$ can be expressed as

$$b(t) = \int_{-\infty}^{\infty} h_r(\lambda)\eta(t - \lambda)d\lambda. \quad (37)$$

The auto correlation function of $b(t)$ is by definition

$$\begin{aligned} \phi_{bb}(\tau) &= \lim_{T \rightarrow \infty} \frac{1}{2T} \int_{-T}^T b(t)b(t + \tau)dt \\ &= \lim_{T \rightarrow \infty} \frac{1}{2T} \int_{-T}^T \int_{-\infty}^{\infty} \int_{-\infty}^{\infty} h_r(\lambda)h_r(\xi)\eta(t - \lambda)\eta(t + \tau - \xi)d\lambda d\xi dt \\ &= \int_{-\infty}^{\infty} \int_{-\infty}^{\infty} h_r(\lambda)h_r(\xi) \left[\lim_{T \rightarrow \infty} \int_{-T}^T \eta(t - \lambda)\eta(t + \tau - \xi)dt \right] d\lambda d\xi \\ &= \int_{-\infty}^{\infty} \int_{-\infty}^{\infty} h_r(\lambda)h_r(\xi)\phi_{nn}(\tau + \lambda - \xi)d\lambda d\xi. \end{aligned} \quad (38)$$

The auto spectral density of $b(t)$, $\Phi_{bb}(\omega)$, is the Fourier transform of $\phi_{bb}(\tau)$, or

$$\Phi_{bb}(\omega) = \int_{-\infty}^{\infty} \phi_{bb}(\tau)e^{-j\omega\tau}d\tau. \quad (39)$$

Using equation (38) for $\phi_{bb}(\tau)$ yields

$$\Phi_{bb}(\omega) = \int_{-\infty}^{\infty} \int_{-\infty}^{\infty} \int_{-\infty}^{\infty} h_r(\lambda)h_r(\xi)\phi_{nn}(\tau + \lambda - \xi)d\lambda d\xi d\tau. \quad (40)$$

Letting $u = \tau + \lambda - \xi$, then $\tau = u + \xi - \lambda$ and

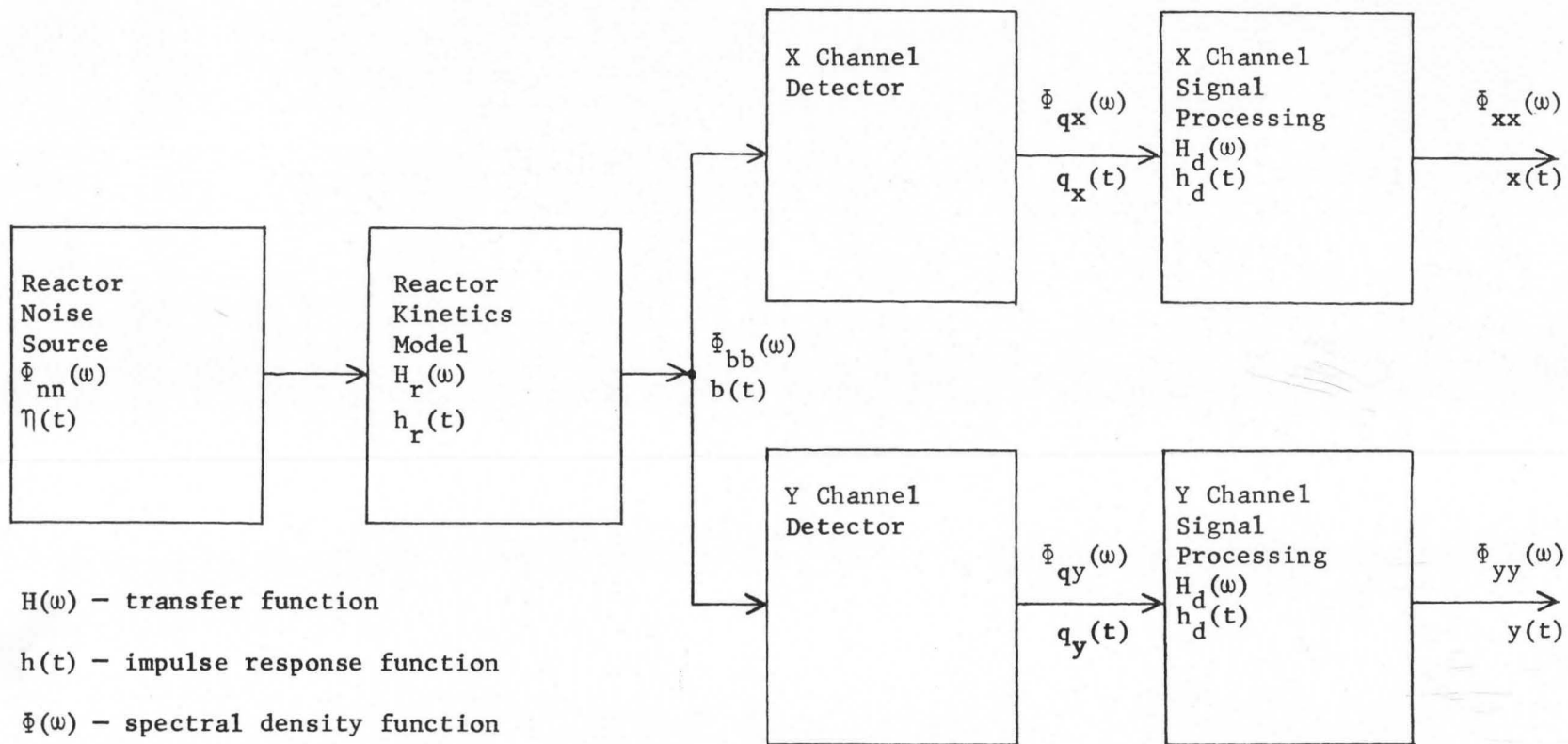


Figure 1. Signal flow diagram.

$$\begin{aligned}
\bar{\Phi}_{bb}(\omega) &= \int_{-\infty}^{\infty} \int_{-\infty}^{\infty} \int_{-\infty}^{\infty} h_r(\lambda) h_r(\xi) \phi_{nn}(\mu) e^{-j\omega(\mu+\xi-\lambda)} d\lambda d\xi d\mu \\
&= \int_{-\infty}^{\infty} h_r(\lambda) e^{+j\omega\lambda} d\lambda \int_{-\infty}^{\infty} h_r(\xi) e^{-j\omega\xi} d\xi \int_{-\infty}^{\infty} \phi_{nn}(\mu) e^{-j\omega\mu} d\mu \\
&= H_r^*(\omega) H_r(\omega) \bar{\Phi}_{nn}(\omega) = |H_r(\omega)|^2 \bar{\Phi}_{nn}(\omega). \tag{41}
\end{aligned}$$

This important result says that the output auto spectral density of a transfer function output is equal to the square modulus of the transfer function times the input auto spectral density.

Cohn [9] states that the spectral output of a detector has two components. The first component is proportional to the input spectrum and may be expressed as

$$\frac{W\bar{q}^2}{l^2} \bar{\Phi}_{bb}(\omega)$$

where

W is the detector efficiency - neutrons detected per fission,

l is again the prompt neutron lifetime,

\bar{q} is the average charge produced per neutron detected,

and

$\bar{\Phi}_{bb}(\omega)$ is the input neutron noise signal auto spectral density.

It should be noted that the detector efficiency, ϵ , used by Cohn [9] is defined as neutrons detected per neutron absorbed. This differs with the definition of detector efficiency, W , used above. For a critical reactor, neutrons detected per neutron absorbed is equal to

the neutrons detected per fission times the average number of neutrons emitted per fission, or $W = \bar{\epsilon}\bar{\nu}$. The second component of the detector output signal is a white noise component which arises from the statistical nature of the detection process. It may be written as

$$\bar{\Phi}_d = \frac{2\bar{q}^{-2}W\bar{\eta}}{\ell}. \quad (43)$$

Hence, the spectral outputs of the detectors shown in Figure 1 are

$$\begin{aligned} \bar{\Phi}_{qx}(\omega) &= \bar{\Phi}_{dx}(\omega) + \frac{W\bar{q}^{2-2}}{\ell^2} \bar{\Phi}_{bb}(\omega) \\ &= \bar{\Phi}_{dx}(\omega) + \frac{W\bar{q}^{2-2}}{\ell^2} |H_r(\omega)|^2 \bar{\Phi}_{nn}(\omega), \end{aligned} \quad (44)$$

and similarly,

$$\bar{\Phi}_{qy}(\omega) = \bar{\Phi}_{dy}(\omega) + \frac{W\bar{q}^{2-2}}{\ell^2} |H_r(\omega)|^2 \bar{\Phi}_{nn}(\omega). \quad (45)$$

It should be noted that $\bar{\Phi}_{dx}(\omega)$ and $\bar{\Phi}_{dy}(\omega)$ are uncorrelated noise sources, even though they have the same magnitude, given in equation (43).

Using a development similar to the one used to arrive at equation (41), the auto spectral densities of the output signals $x(t)$ and $y(t)$ shown in Figure 1 are easily shown to be

$$\begin{aligned} \bar{\Phi}_{xx}(\omega) &= |H_d(\omega)|^2 \bar{\Phi}_{qx}(\omega) \\ &= |H_d(\omega)|^2 \left\{ \bar{\Phi}_{dx}(\omega) + \frac{W\bar{q}^{2-2}}{\ell^2} |H_r(\omega)|^2 \bar{\Phi}_{nn}(\omega) \right\}, \end{aligned} \quad (46)$$

and similarly,

$$\bar{\Phi}_{yy}(\omega) = |H_d(\omega)|^2 \left\{ \bar{\Phi}_{dy}(\omega) + \frac{W\bar{q}^{2-2}}{\ell^2} |H_r(\omega)|^2 \bar{\Phi}_{nn}(\omega) \right\}. \quad (47)$$

In equations (44) and (45) the second term is the reactor noise contribution to Φ_{qx} , while the first term is the detection noise contribution. A ratio of correlated reactor noise to uncorrelated detection noise can be defined as

$$Q^c(\omega) = \frac{\frac{W^2 \eta^2}{\ell^2} |H_r(\omega)|^2 \Phi_{nn}}{\Phi_d(\omega)} \quad (48)$$

which upon substitution of equations (15), (36), and (43) reduces to

$$Q^c(\omega) = \frac{WD/\beta^2}{1 + (\omega/\alpha_c)^2} = \frac{Q_{\max}^c}{1 + (\omega/\alpha_c)^2} \quad (49)$$

where

$$Q_{\max}^c = \frac{WD}{\beta^2} \quad (50)$$

When the effects of the statistical nature of the detection chamber ionization process are included, as was done by Seifritz [19], the maximum ratio of reactor noise to detection noise is reported as

$$Q_{\max}^c = \frac{WD}{R\beta^2} \quad (51)$$

where R is the "Bennett factor" which is dependent on ionization statistics. In either case, the importance of detector efficiency in making the correlated reactor noise signal observable above the uncorrelated detection noise in the auto spectral density $\Phi_{xx}(\omega)$ or $\Phi_{yy}(\omega)$ is apparent since the ratio is directly proportional to W , the detector efficiency.

E. Cross Spectral Density

It has been previously mentioned that the use of two detection systems can allow the rejection of the random detection system noise. This fact is evident in the formulation of the cross spectral density function given below. Figure 2 shows two identical detection signal processing systems which have as inputs the sum of a common signal, $i(t)$, and an uncorrelated signal, $Z(t)$, for each channel. Note that $i(t)$, $Z_m(t)$, and $Z_n(t)$ have no correlation with each other. When the convolution integral is applied, it is found that

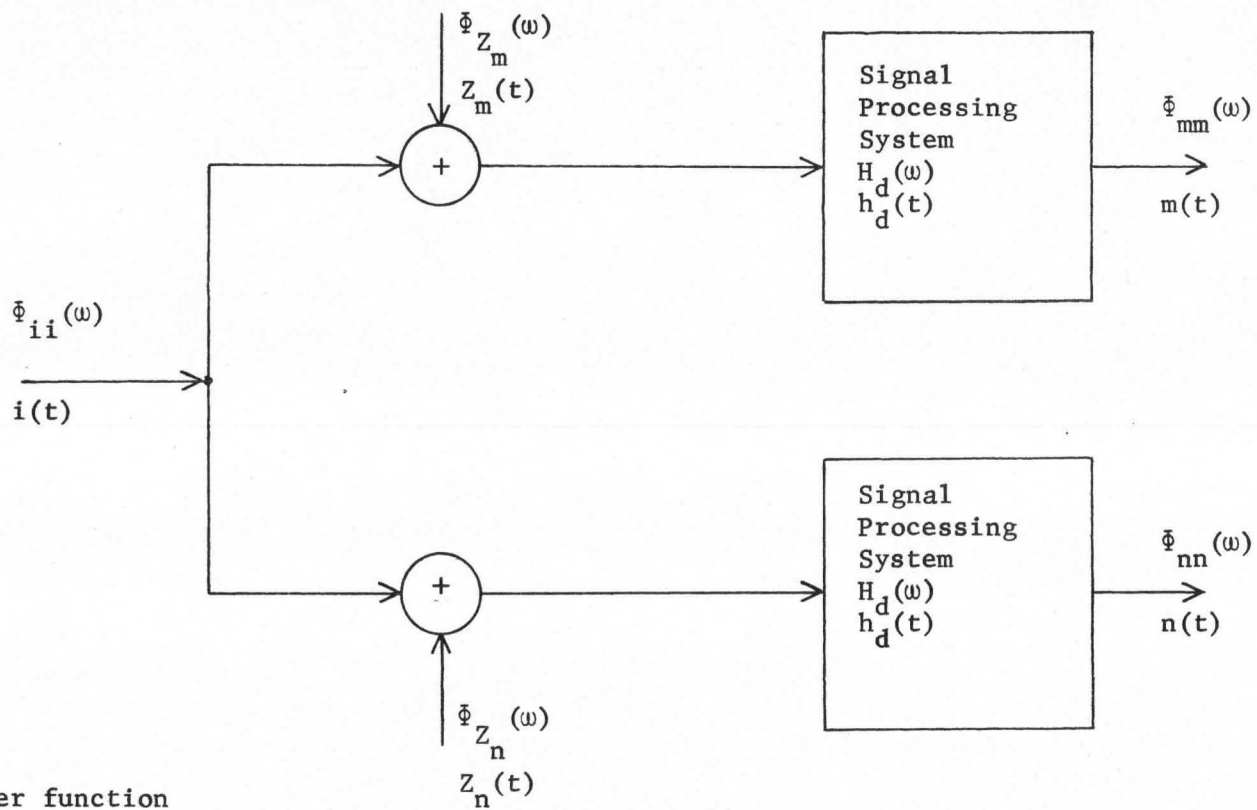
$$m(t) = \int_{-\infty}^{\infty} h_d(u) [Z_m(t-u) + i(t-u)] du \quad (52)$$

and

$$n(t) = \int_{-\infty}^{\infty} h_d(v) [Z_n(t-v) + i(t-v)] dv . \quad (53)$$

The cross correlation function of $m(t)$ and $n(t)$ is

$$\begin{aligned} \phi_{mn}(\tau) &= \lim_{T \rightarrow \infty} \frac{1}{2T} \int_{-T}^T m(t)n(t+\tau) dt \\ &= \lim_{T \rightarrow \infty} \frac{1}{2T} \int_{-T}^T \int_{-\infty}^{\infty} \int_{-\infty}^{\infty} h_d(u) h_d(v) [Z_m(t-u) + i(t-u)] \\ &\quad \times [Z_n(t+\tau-v) + i(t+\tau-v)] du dv dt \\ &= \lim_{T \rightarrow \infty} \frac{1}{2T} \int_{-T}^T \int_{-\infty}^{\infty} \int_{-\infty}^{\infty} h_d(u) h_d(v) [Z_m(t-u) Z_n(t+\tau-v) \\ &\quad + Z_m(t-u) i(t+\tau-v) + i(t-u) Z_n(t+\tau-v) \end{aligned}$$



$H(\omega)$ - transfer function

$h(t)$ - impulse response function

$\Phi(\omega)$ - spectral density function

Figure 2. Signal processing system.

$$\begin{aligned}
& + i(t - u)i(t + \tau - v)]dudvdt \\
= & \int_{-\infty}^{\infty} \int_{-\infty}^{\infty} h_d(u)h_d(v) \left\{ \lim_{T \rightarrow \infty} \frac{1}{2T} \int_{-T}^T [Z_m(t - u)Z_n(t + \tau - v) \right. \\
& + Z_m(t - u)i(t + \tau - v) + i(t - u)Z_n(t + \tau - v) \\
& \left. + i(t - u)i(t + \tau - v)]dt \right\} dudv \\
= & \int_{-\infty}^{\infty} \int_{-\infty}^{\infty} h_d(u)h_d(v) [\phi_{zmzn}(\tau + u - v) + \phi_{zmi}(\tau + u - v) \\
& + \phi_{izn}(\tau + u - v) + \phi_{ii}(\tau + \mu - v)]dudv. \quad (54)
\end{aligned}$$

Since $i(t)$, $Z_m(t)$, and $Z_n(t)$ are uncorrelated, ϕ_{zmzn} , ϕ_{zmi} , and ϕ_{izn} are equal to zero, leaving the cross correlation of $m(t)$ and $n(t)$

as

$$\phi_{mn}(\tau) = \int_{-\infty}^{\infty} \int_{-\infty}^{\infty} h_d(u)h_d(v)\phi_{ii}(\tau + u - v)dudv. \quad (55)$$

The cross spectral density function is the Fourier transform of the cross correlation function, or

$$\begin{aligned}
\bar{\Phi}_{mn}(\omega) &= \int_{-\infty}^{\infty} \phi_{mn}(\tau)e^{-j\omega\tau}d\tau \\
&= \int_{-\infty}^{\infty} \int_{-\infty}^{\infty} \int_{-\infty}^{\infty} h_d(u)h_d(v)\phi_{ii}(\tau + \mu - v)e^{-j\omega\tau}dudvd\tau. \quad (56)
\end{aligned}$$

If a change in variables is made, $\Delta = \tau + u - v$, then $\tau = \Delta + v - u$

and

$$\begin{aligned}
\bar{\Phi}_{mn}(\omega) &= \int_{-\infty}^{\infty} \int_{-\infty}^{\infty} \int_{-\infty}^{\infty} h_d(u) h_d(v) \phi_{ii}(\Delta) e^{-j\omega(\Delta+v-u)} du dv d\Delta \\
&= \int_{-\infty}^{\infty} h_d(u) e^{+j\omega u} du \int_{-\infty}^{\infty} h_d(v) e^{-j\omega v} dv \int_{-\infty}^{\infty} \phi_{ii}(\Delta) e^{-j\omega\Delta} d\Delta \\
&= H_d^*(\omega) H_d(\omega) \bar{\Phi}_{ii}(\omega) = |H_d(\omega)|^2 \bar{\Phi}_{ii}(\omega) \quad . \quad (57)
\end{aligned}$$

Note that the output cross spectral density function is dependent only on the square modulus of the transfer function and the common input power spectral density function, and is independent of the two uncorrelated signal inputs. Applying these results to the cross spectral density of the two output signals shown in Figure 1, it will be recalled that $\bar{\Phi}_{qx}(\omega)$ and $\bar{\Phi}_{qy}(\omega)$ as expressed in equations (44) and (45) contain a common spectrum of

$$\frac{W^2 q^2}{\ell^2} |H_r(\omega)|^2 \bar{\Phi}_{nn}(\omega) \quad (58)$$

and uncorrelated components of $\bar{\Phi}_{dx}(\omega)$ and $\bar{\Phi}_{dy}(\omega)$ respectively. The resulting cross spectral density function of the two output signals shown in Figure 1 is therefore

$$\bar{\Phi}_{xy}(\omega) = \frac{W^2 q^2}{\ell^2} |H_r(\omega)|^2 |H_d(\omega)|^2 \bar{\Phi}_{nn}(\omega) \quad (59)$$

and is independent of $\bar{\Phi}_{dx}(\omega)$ and $\bar{\Phi}_{dy}(\omega)$.

F. Coherence Function

The inherent advantage of the coherence function is that it is independent of the detection system transfer function, $H_d(\omega)$, shown

in Figures 1 and 2. Since the auto and cross spectral density functions contain $H_d(\omega)$ as a variable, this detection system transfer function must be determined before either the auto or the cross spectral density can independently be used to determine relationships among reactor parameters. If, however, the auto and cross spectral densities are combined in the form of the coherence function, $\rho(\omega)$, defined as

$$\rho(\omega) = \frac{\Phi_{xy}(\omega)}{[\Phi_{xx}(\omega)\Phi_{yy}(\omega)]^{1/2}}, \quad (60)$$

and equations (46), (47), and (59) are inserted to give

$$\rho(\omega) = \frac{\frac{Wq^{2-2}}{\ell^2} |H_r(\omega)|^2 \Phi_{nn}(\omega)}{\left\{ \left[\Phi_{dx}(\omega) + \frac{Wq^{2-2}}{\ell^2} |H_r(\omega)|^2 \Phi_{nn}(\omega) \right] \left[\Phi_{dy}(\omega) + \frac{Wq^{2-2}}{\ell^2} |H_r(\omega)|^2 \Phi_{nn}(\omega) \right] \right\}^{1/2}}, \quad (61)$$

it is evident that $\rho(\omega)$ is independent of $H_d(\omega)$. If $\Phi_{nn}(\omega)$, $H_r(\omega)$, $\Phi_{dx}(\omega)$, and $\Phi_{dy}(\omega)$ are replaced by equations (15), (36), and (43), and the identity for Q_{\max}^c is used, $\rho(\omega)$ can be reduced to

$$\rho(\omega) = \frac{Q_{\max}^c}{1 + Q_{\max}^c + (\omega/\alpha_c)^2}. \quad (62)$$

A "Bode plot" (log amplitude vs. log frequency) of equation (62) indicates that the coherence function has a low frequency plateau value of

$$\rho_o = \rho(\omega \ll \alpha_c) = \frac{Q_{\max}^c}{1 + Q_{\max}^c}, \quad (63)$$

and a break frequency of

$$\omega_{\beta} = \alpha_c [1 + Q_{\max}^c]^{1/2} . \quad (64)$$

Combining equations (64) and (63) and solving for α_c yields

$$\alpha_c = \omega_{\beta} [1 - \rho_o]^{1/2} . \quad (65)$$

Therefore, if the coherence function is known, the prompt neutron decay constant, α_c , can be determined.

III. DETERMINATION OF THE COHERENCE FUNCTION BY POLARITY CORRELATION

A. Overall System

Up to this point the discussion has involved explaining how the coherence function relates to the prompt neutron decay constant. The coherence function may then be evaluated in the traditional way by finding the auto and cross spectral density functions, or it may be evaluated by the method of polarity correlation demonstrated by Seifritz [19]. A system diagram of this type of polarity correlation is shown in Figure 3. The two input neutron noise signals $x(t)$ and $y(t)$ are the same signals that are shown as output signals in Figure 1. These two neutron noise signals are filtered by variable frequency narrow pass-band filters and fed into a polarity correlator. The polarity correlator determines the signs of the two signals with respect to their mean values, compares these signs, and outputs either a + 1 or - 1 logic state as shown in Table I. This polarity correlator output, $C_{\omega}(t)$, is time averaged by using it to drive an "AND" circuit in conjunction with a 100KHz square wave and then counting the "AND" output for a specified period of time. The average output is given by

$$\overline{C_{\omega}(t)} = \left[\frac{2(\text{counts recorded out of "AND"})}{(\text{total no. of 100KHz counts})} \right] - 1. \quad (66)$$

The following shows that $\overline{C_{\omega}(t)}$ yields the coherence function directly.

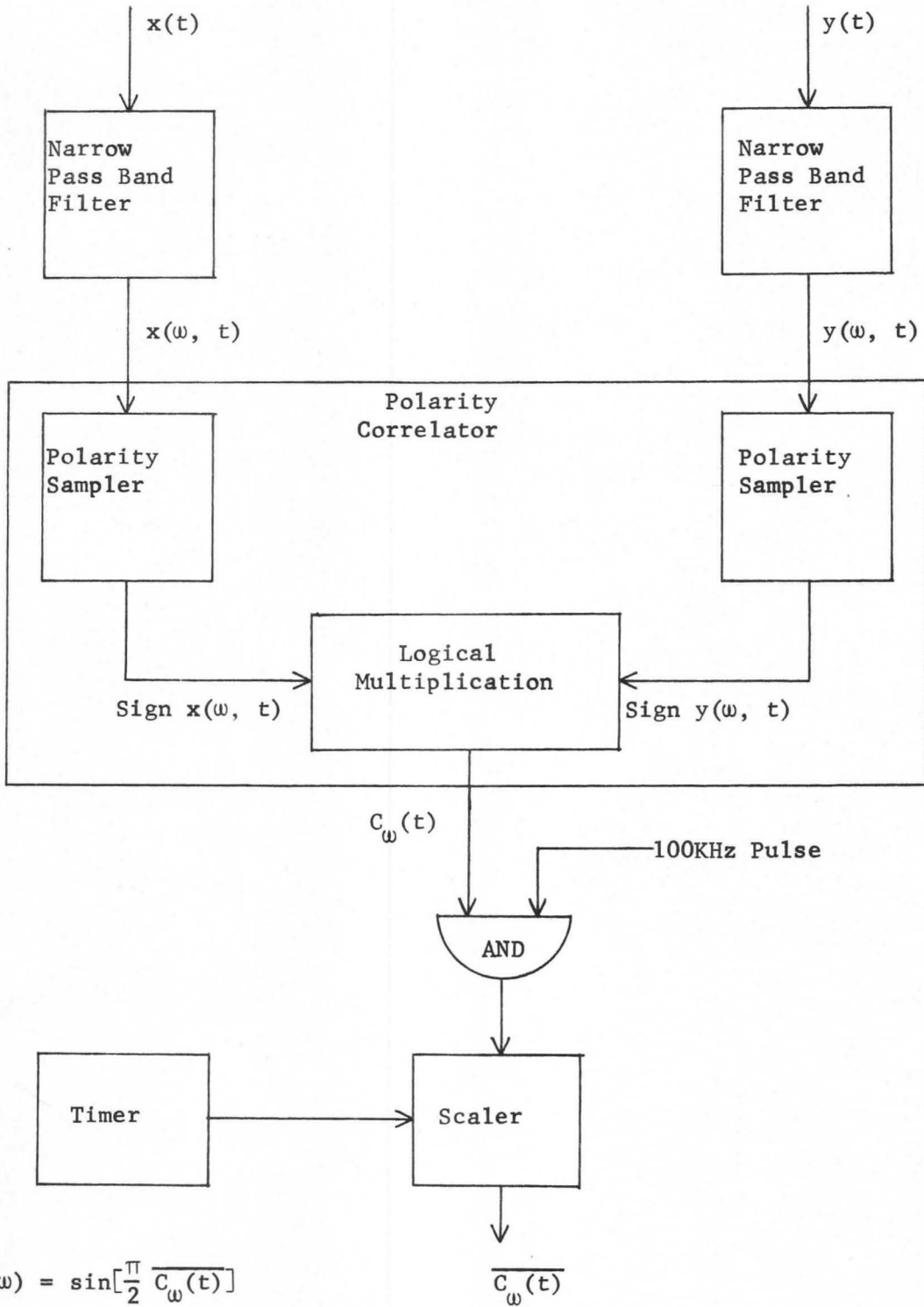


Figure 3. A polarity correlation system.

Table I. Polarity correlator output

Sign of $x(\omega, t)$ with respect to $x(\omega, t)$	+	+	-	-
Sign of $y(\omega, t)$ with respect to $y(\omega, t)$	+	-	+	-
Logic state of correlator output $C_\omega(t)$	+ 1	- 1	- 1	+ 1

B. Theory of Coherence Function Determination

Seifritz [19] notes that if $\overline{x(\omega, t)}$ and $\overline{y(\omega, t)}$ are equal to zero, the joint probability density function of $x(\omega, t)$ and $y(\omega, t)$ is

$$f(x, y) = \left\{ \frac{1}{2\pi x^2 y^2 \sqrt{1 - \rho^2(\omega)}} \right\}^{-1} \text{EXP} \left\{ \frac{1}{2[1 - \rho^2(\omega)]} \right. \\ \left. \times \left[\frac{x^2}{x^2} - \frac{2\rho(\omega)xy}{x^2 y^2} + \frac{y^2}{y^2} \right] \right\} \quad (67)$$

where $\rho(\omega)$ is the coherence function of $x(\omega, t)$ and $y(\omega, t)$. The above joint probability density function may be thought of as a Gaussian shaped "mountain" above the xy plane with unity volume and centered at the origin. The appropriate assumption made in arriving at equation (67) was that $x(\omega, t)$ and $y(\omega, t)$ were normal or Gaussian random noise signals, which has been found to be the case.

The output of the correlator is shown in Figure 3 as $C_\omega(t)$ with either a + 1 or - 1 logic state depending on the signs of $x(\omega, t)$

and $y(\omega, t)$ as shown in Table I. The probability that $C_\omega(t)$ will be in the + 1 logic state, $P_{\omega+}$, can be found by integrating the volume of $f_\omega(x, y)$ above the area in the xy plane where $x(\omega, t)$ and $y(\omega, t)$ are both positive or both negative. Integrating over the first and third quadrants yields

$$P_{\omega+} = \int_0^\infty \int_0^\infty f_\omega(x, y) dx dy + \int_{-\infty}^0 \int_{-\infty}^0 f_\omega(x, y) dx dy$$

$$= \frac{\pi + 2 \text{ArcSin } \rho(\omega)}{2\pi} \quad (68)$$

The probability that $C_\omega(t)$ will have a - 1 logic state, $P_{\omega-}$, can be found in like manner by integrating over the second and fourth quadrants resulting in

$$P_{\omega-} = \int_{-\infty}^0 \int_0^\infty f_\omega(x, y) dx dy + \int_0^\infty \int_{-\infty}^0 f_\omega(x, y) dx dy$$

$$= \frac{\pi - 2 \text{ArcSin } \rho(\omega)}{2\pi} \quad (69)$$

The time average of $C_\omega(t)$ is

$$\overline{C_\omega(t)} = P_{\omega+} - P_{\omega-} = \frac{2}{\pi} \text{ArcSin } \rho(\omega), \quad (70)$$

or solving for the coherence function gives

$$\rho(\omega) = \text{Sin}\left[\frac{\pi}{2} \overline{C_\omega(t)}\right]. \quad (71)$$

Therefore, by selecting various frequencies with the variable frequency narrow pass-band filters shown in Figure 3, the coherence function as a function of frequency can be determined by equation (71), and the

prompt neutron decay constant, α_c , is then found by the use of equation (65).

IV. APPLICATION OF DYNAMIC FILTERING

A. Theory of Dynamic Filtering

The basis for dynamic (heterodyne) filtering is the linear modulation process by which a frequency spectrum can be shifted in frequency. This allows the building of a "variable center frequency" bandpass filtering system which consists of a fixed frequency filter and a linear modulator to shift the incoming signal by a variable amount in frequency to make the fixed frequency filter appear variable. Any linear modulator will perform the frequency shift required, but for reason of spectral content of the output which is discussed later, a balanced modulator in the form of a "bipolar chopper" appears to be the most suited to the application of dynamic filtering in polarity correlation.

The waveforms of a "bipolar chopper" are shown in Figure 4. It is apparent that the output signal is simply the input signal alternatively sampled or "chopped" at the positive and negative values of its amplitude. The output signal may be written as

$$O(t) = i(t)S(t), \quad (72)$$

where $i(t)$ is the input signal as a function of time, and $S(t)$ is the square wave carrier signal.

The analysis of the spectral content of the output signal begins by showing the result of multiplying two sinusoidal signals. If $W(t)$ is the product of two sinusoids,

$$W(t) = A_1 \cos(\omega_1 t + \theta_1) \cdot A_2 \cos(\omega_2 t + \theta_2), \quad (73)$$

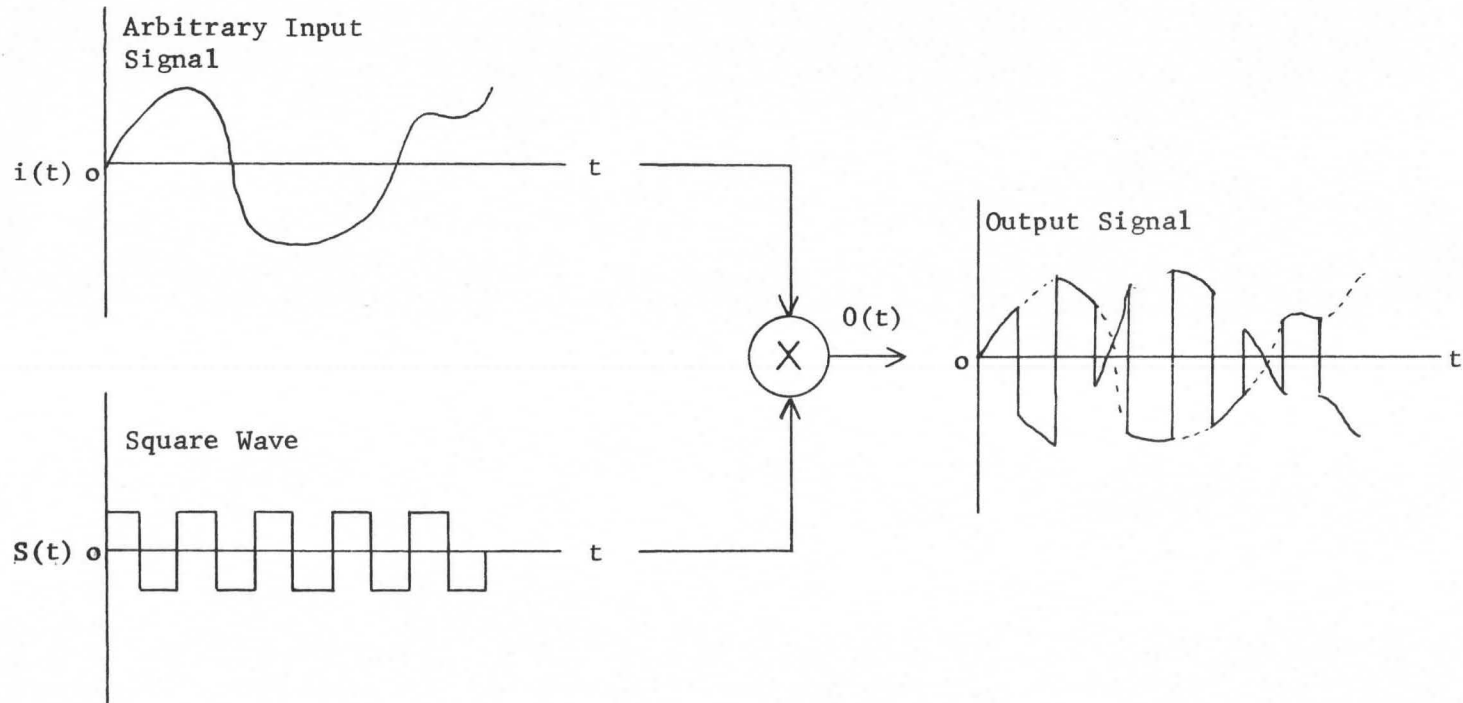


Figure 4. Bipolar chopper waveforms.

which by trigometric identity is

$$\begin{aligned}
 W(t) = & \frac{A_1 A_2}{2} \text{Cos}[(\omega_1 + \omega_2)t + (\theta_1 + \theta_2)] \\
 & + \frac{A_1 A_2}{2} \text{Cos}[(\omega_1 - \omega_2)t + (\theta_1 - \theta_2)], \quad (74)
 \end{aligned}$$

indicating that the multiplication of two sinusoids results in two new sinusoids at frequencies equal to the sum and difference of the original two frequencies. If this argument is extended to the case of the multiplication of the signals in equation (72), each of which may contain a whole spectrum of frequencies, the resulting output spectrum contains the sum and difference frequencies of every possible product of the frequency components of the two multiplied signals. By a simple Fourier series representation of $S(t)$, the zero mean square wave spectrum can be shown to be as indicated in Figure 5b. The sum and difference frequency of all possible component products between the assumed input spectrum, Figure 5a, and the square wave spectrum results in the bipolar output spectrum shown in Figure 5c.

For comparison, Figure 6 shows the output spectra of an amplitude modulator and a unipolar chopper form of balanced modulator as shown by Carlson [7] and Schwartz [18] respectively. Note that the spectral contents of the unipolar and bipolar outputs are identical except for the original input spectral content (baseband signal) included in the unipolar output.

Figure 7 illustrates the location of the center frequency for the fixed frequency filter. As the carrier frequency is lowered,

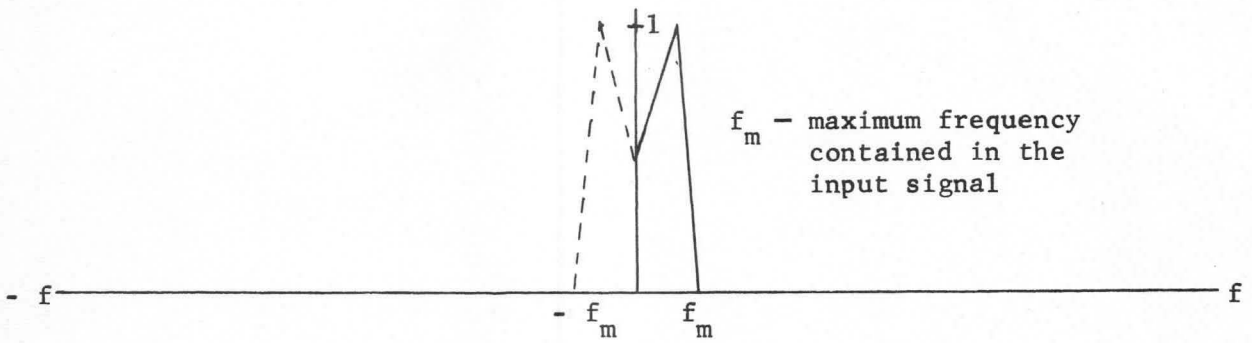


Figure 6a. Assumed input spectra.

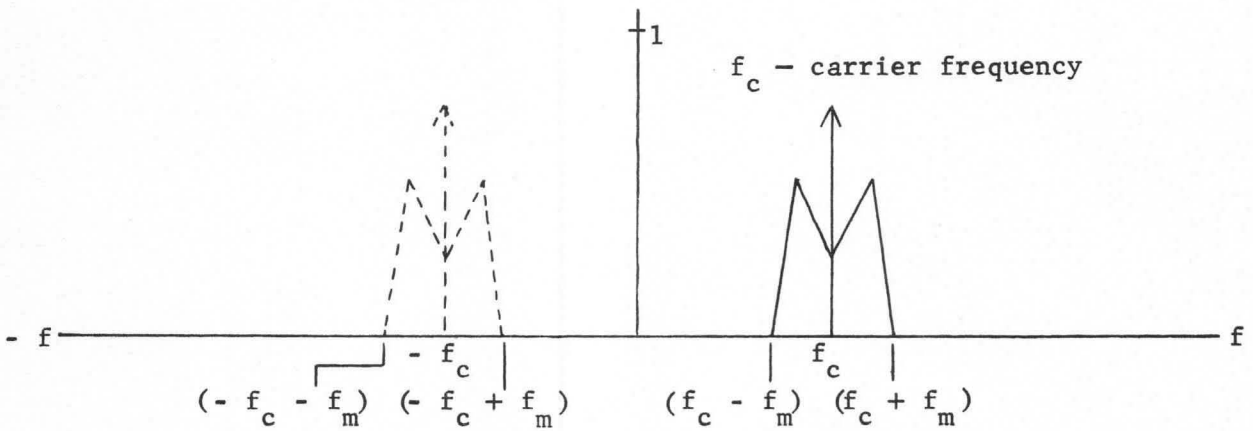


Figure 6b. Amplitude modulator output spectrum

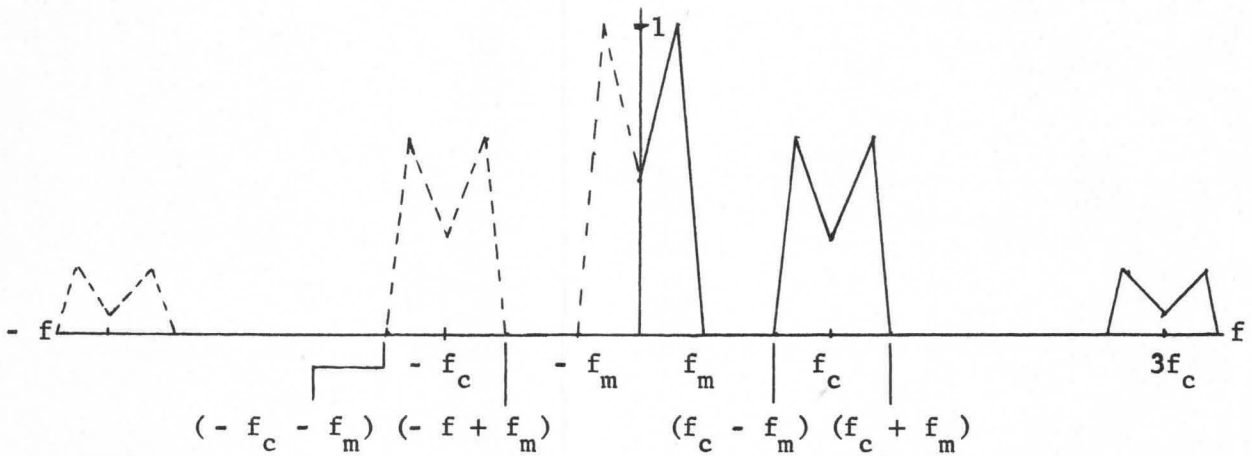


Figure 6c. Unipolar chopper output spectrum.

Figure 6. Modulator spectra.

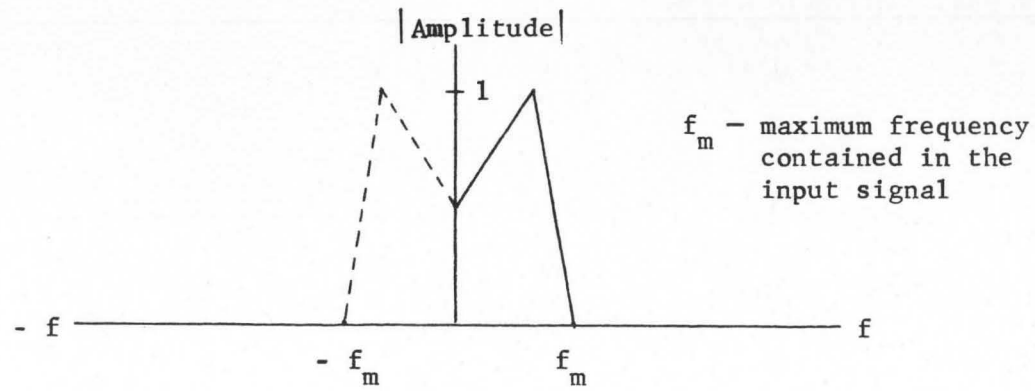


Figure 7a. Assumed input spectrum.

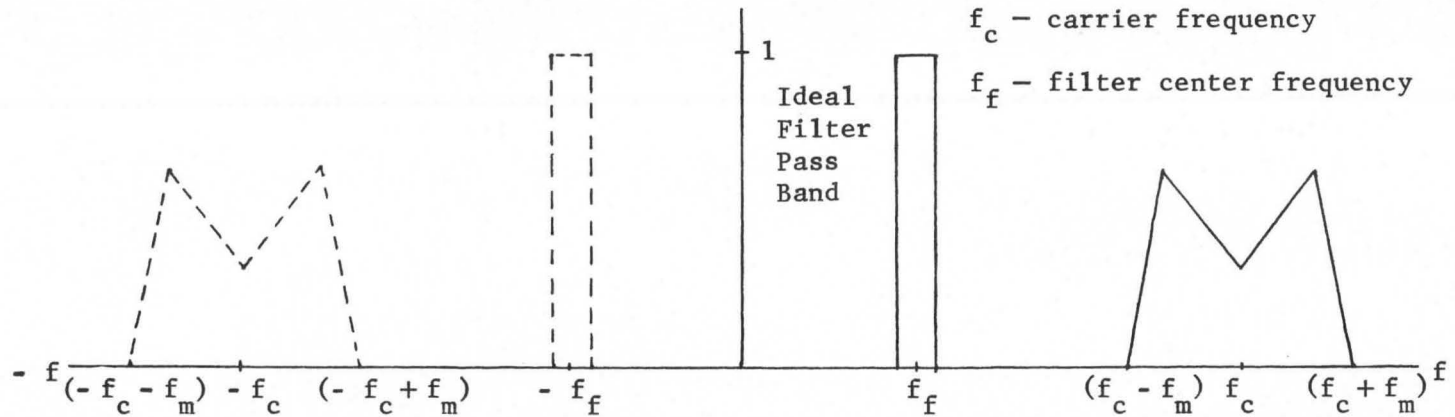


Figure 7b. Filter pass band in output spectrum.

Figure 7. Location of filter pass band in the bipolar chopper output spectrum.

selected components of the "lower side band" are placed in the pass band of the filter.

The advantages of the bipolar chopper are now easily pointed out. Since the base band signal is not present in the bipolar output spectrum, the center frequency of the filter may be set at a lower frequency with the bipolar chopper than with the unipolar chopper. A lower center frequency allows the same selectivity, in Hz of bandwidth, with a lower "Q" filter. The "Q" of a filter is defined as the bandwidth divided by the center frequency, or $Q = f/\Delta f$. The advantage of a lower "Q" filter is also shared with the amplitude modulator (AM), but the AM output spectrum contains a strong carrier frequency component which could mask the very lowest frequency components of the input spectrum (those nearest the carrier frequency). An additional advantage of the bipolar chopper is its circuit simplicity.

In theory, the center frequency of the fixed filter used with a bipolar chopper may be chosen (neglecting filter bandwidth) as low as one half of the maximum frequency contained in the input spectrum. Any lower center frequency would result in inaccurate levels being recorded for low frequencies in the input spectrum, for the "frequency fold over" discussed by Bennett [5] would allow the highest frequency components to pass through the filter with the low frequency components.

In actual practice, a "guard band" of frequency is needed to allow for the filter bandwidth, the filter skirts, and signals which are not band limited. The maximum frequency contained in the input spectrum appears to be a practical minimum for the fixed filter

center frequency in a polarity correlation dynamic filtering system.

B. Advantages of Dynamic Filtering

The two narrow pass band filters shown in Figure 3 may be independent tunable filters, but care must be taken to assure that both filters have been set to the same center frequency. For a large number of data points this tuning procedure can become quite tedious.

With a dynamic filtering system, each signal is fed into a modulator followed by a fixed frequency filter. The filters are aligned permanently to the same center frequency, and then a common carrier frequency is used to drive both modulators resulting in matching filter pass band locations at all filtering frequencies. A change in filtering frequency requires only a change in the carrier frequency.

The dynamic filter also has the capability of better resolving power or selectivity, since a narrow bandwidth, sharp skirted, fixed filter is easier to build than a variable frequency filter with similar performance.

C. Requirements of a Polarity Correlation Filtering System

The range of frequencies that the filtering system is required to process can be estimated from equation (64). For U^{235} fueled thermal reactors and average detector efficiencies, the coherence function break frequencies are typically in the 5-50 Hz range. Information

on the coherence function amplitude is needed to at least a decade above the break frequency, resulting in needed filtering capability up to approximately 500 Hz for a typical thermal reactor application. If the incoming neutron noise signal is band limited to this frequency the center frequency of the filter can be chosen at this frequency as discussed in the previous section.

The bandwidth, or "Q", of the filter is chosen as a compromise between increased selectivity for accurate determination of the coherence function and the expense of the filter. The minimum bandwidth of the filter is also limited by requiring reasonable data collection times. As the bandwidth decreases when filtering random noise, the output must be monitored for a longer period of time to insure an accurate measurement. A bandwidth of 5 Hz appears to be a good compromise value for a thermal reactor application.

The sharpness of the filter skirts required is determined by the coherence function roll-off. A "Bode plot" of equation (62) shows the coherence function to be decreasing in amplitude at 20db/decade above the break frequency. The filter roll-off should be sharper than this.

An additional requirement of the filter is a large amount of out-of-band attenuation. This is required to reject all of the odd carrier harmonic spectra included in the bipolar chopper output shown in Figure 5c. A minimum of 60db of attenuation at all out-of-band frequencies is needed.

V. CONCLUDING REMARKS

This study has reviewed the theory of the polarity correlation technique as used in the determination of the prompt neutron decay constant, α_c . In the theory it was shown that the polarity correlation technique was used to determine the coherence function, which in turn yielded the prompt neutron decay constant. The use of the coherence function highlights one of the advantages of polarity correlation, for it will be recalled that the coherence function has been shown to be independent of the signal processing equipment transfer functions. Because of this independence, the polarity correlation technique requires no corrections to accommodate variations in processing equipment frequency response; a fact that becomes very important when measurements are made on fast reactors where higher frequency signal processing is required.

The review of polarity correlation theory has also shown that a polarity correlation system uses only the signs of the signals for information processing, making the system after the polarity sampling process a digital or logical system. Many commonly available and relatively inexpensive commercial logic packages can be used in the implementation of the system, and the range of external digital processing equipment to which the polarity correlation system could be mated is quite large.

The application of dynamic filtering in a polarity correlation system was also presented. The advantages of faster data collection procedures and better selectivity were pointed out.

In summary, the polarity correlation technique of reactor noise analysis has sufficient advantages over more conventional analog techniques to insure that it will become an increasingly popular method of noise analysis particularly in fast reactor applications.

VI. BIBLIOGRAPHY

1. R. BADGLEY and R. UHRIG, Nuc. Sci. and Eng., 19, 158 (1964).
2. J. BALCOMB, in Noise Analysis in Nuclear Systems, pp. 183-201, Proceedings of the Symposium, Gainesville, Florida (1963).
3. J. BALCOMB, H. DEMUTH, and E. GYFTOPOULOUS, Nuc. Sci. and Eng., 9, 159 (1961).
4. J. S. BENDAT, Principles and Applications of Random Noise Theory, Chap. 1, Wiley and Sons, Inc., New York (1958).
5. W. R. BENNETT, Introduction to Signal Transmission, p. 182, McGraw-Hill, New York (1970).
6. R. G. BROWN and J. W. NILSSON, Introduction to Linear Systems Analysis, pp. 78-247, Wiley and Sons, Inc., New York (1962).
7. A. B. CARLSON, Communication Systems: An Introduction to Signals and Noise in Electrical Communication, p. 170, McGraw-Hill, New York (1968).
8. C. E. COHN, Nuc. Sci. and Eng., 5, 331 (1959).
9. C. E. COHN, Nuc. Sci. and Eng., 7, 472 (1960).
10. R. DANOFSKY, in Noise Analysis in Nuclear Systems, pp. 229-248, Proceedings of the Symposium, Gainesville, Florida (1963).
11. W. B. DAVENPORT and W. L. ROOT, Introduction to Random Signals and Noise, Chap. 7, McGraw-Hill, New York (1958).
12. J. B. DRAGT, in Neutron Noise, Waves, and Pulse Propagation, pp. 47-48, Transactions of the Symposium, Gainesville, Florida (1966).
13. J. B. DRAGT, Nukleonik, 8, 188 (1966).
14. S. GLASSTONE and A. SESONSKE, Nuclear Reactor Engineering, pp. 297-298, D. Van Nostrand, Princeton, New Jersey (1967).
15. R. C. KRYTER, D. N. FRY, and D. P. ROUX, Trans. Am. Nuc. Soc., 10, 283 (1967).
16. N. PACILIO, Nuc. Sci. and Eng., 35, 249 (1969).
17. V. RAJAGOPAL, Nuc. Sci. and Eng., 12, 218 (1962).

18. M. SCHWARTZ, Information Transmission, Modulation, and Noise, p. 165, McGraw-Hill, New York (1959).
19. W. SEIFRITZ, Nuc. Appl. and Tech., 7, 513 (1969).
20. W. SEIFRITZ and D. STEGEMANN, Nukleonik, 9, 169 (1967).
21. W. SEIFRITZ, D. STEGEMANN, and W. VATH, in Neutron Noise, Waves, and Pulse Propagation, p. 40, Transactions of the Symposium, Gainesville, Florida (1966).
22. T. E. STERN, in Noise Analysis in Nuclear Systems, pp. 203-215, Proceedings of the Symposium, Gainesville, Florida (1963),
23. R. E. UHRIG, Random Noise Techniques in Nuclear Reactor Systems, pp. 83-110, Ronald Press, New York (1970).
24. J. VALAT, in Noise Analysis in Nuclear Systems, pp. 219-228, Proceedings of the Symposium, Gainesville, Florida (1963).

VII. ACKNOWLEDGMENTS

The author is indebted to his major professor, Dr. Richard A. Hendrickson, for the suggestion of topic and guidance he provided in this study.

The financial assistance received from the National Science Foundation and the National Defense Education Act is gratefully acknowledged.

Finally, deep appreciation is extended to the author's wife, Sharon, and daughter, Deborah, for their sacrifices and support during this investigation.